

## Supplementary information

### Enhanced energy storage properties of Hafnium-modified (0.7Ba<sub>0.55</sub>Sr<sub>0.45</sub>-0.3Bi<sub>0.5</sub>Na<sub>0.5</sub>)TiO<sub>3</sub>-based relaxor ferroelectric ceramics via regulating polarization nonlinearity and bandgap

Fan Yang<sup>a,c</sup>, Yizheng Bao<sup>a</sup>, Wei Huang<sup>a,c,d</sup>, Xin Li<sup>a</sup>, Ying Chen<sup>a,c,\*</sup>, and Genshui Wang<sup>a,b,c,\*</sup>

<sup>a</sup> Key Laboratory of Inorganic Functional Materials and Devices, Shanghai Institute of Ceramics, Chinese Academy of Sciences, 1295 Dingxi Road, Shanghai 200050, People's Republic of China.

<sup>b</sup> State Key Laboratory of High Performance Ceramics and Superfine Microstructure, Shanghai Institute of Ceramics, Chinese Academy of Sciences, 1295 Dingxi Road, Shanghai 200050, People's Republic of China

<sup>c</sup> Center of Materials Science and Optoelectronics Engineering, University of Chinese Academy of Sciences, Beijing 100049, People's Republic of China

<sup>d</sup> School of Physical Science and Technology, ShanghaiTech University, Shanghai 200050, People's Republic of China

\*Corresponding authors:

Prof. Genshui Wang, and Prof. Ying Chen

E-mail: genshuiwang@mail.sic.ac.cn, and chenying@mail.sic.ac.cn

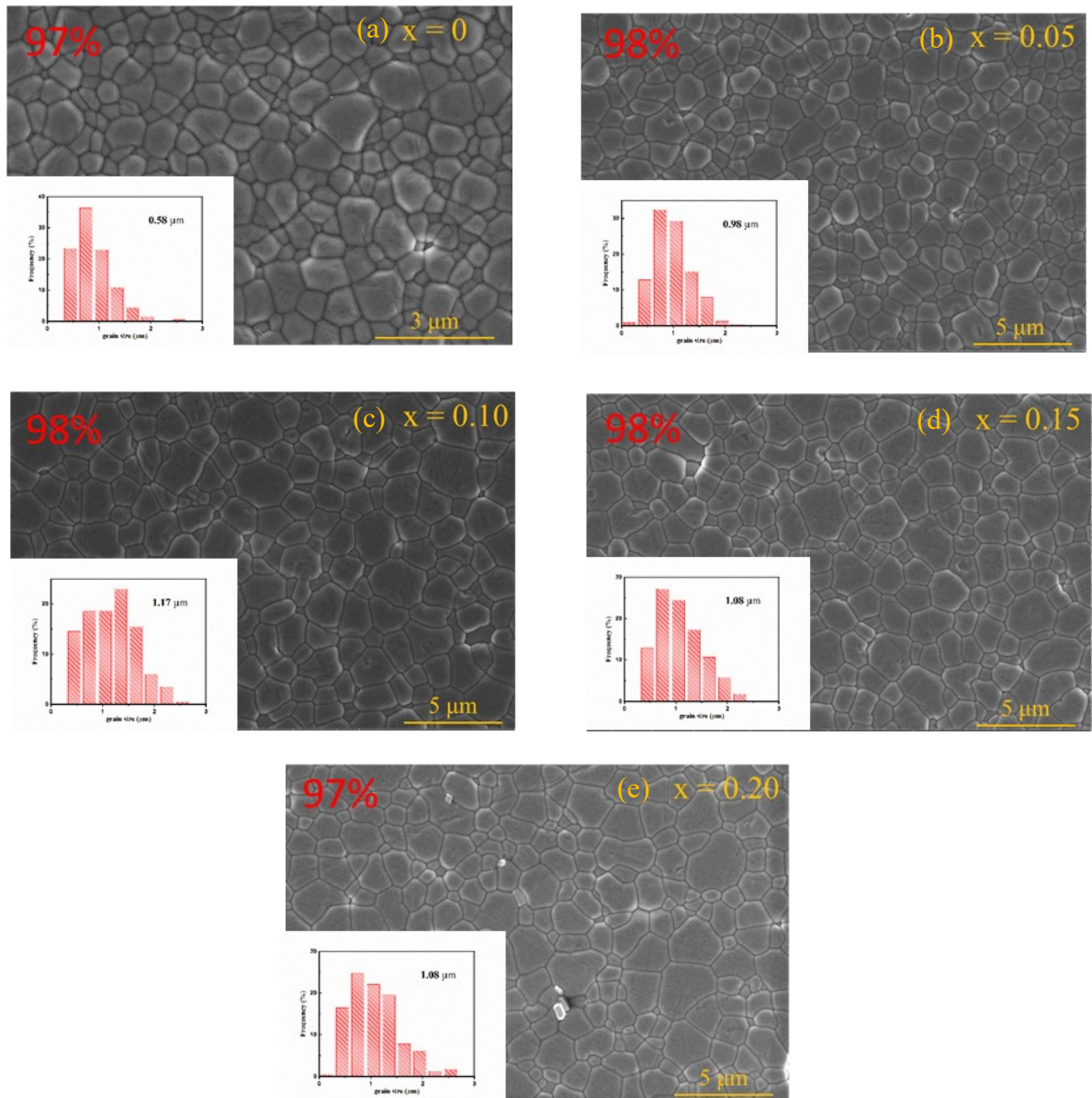


**Fig. S1** The SEM micrographs of the polished and thermal-etched surfaces: (a)  $x=0$ , (b)  $x=0.05$ , (c)  $x=0.10$ , (d)  $x=0.15$ , (e)  $x=0.20$ .

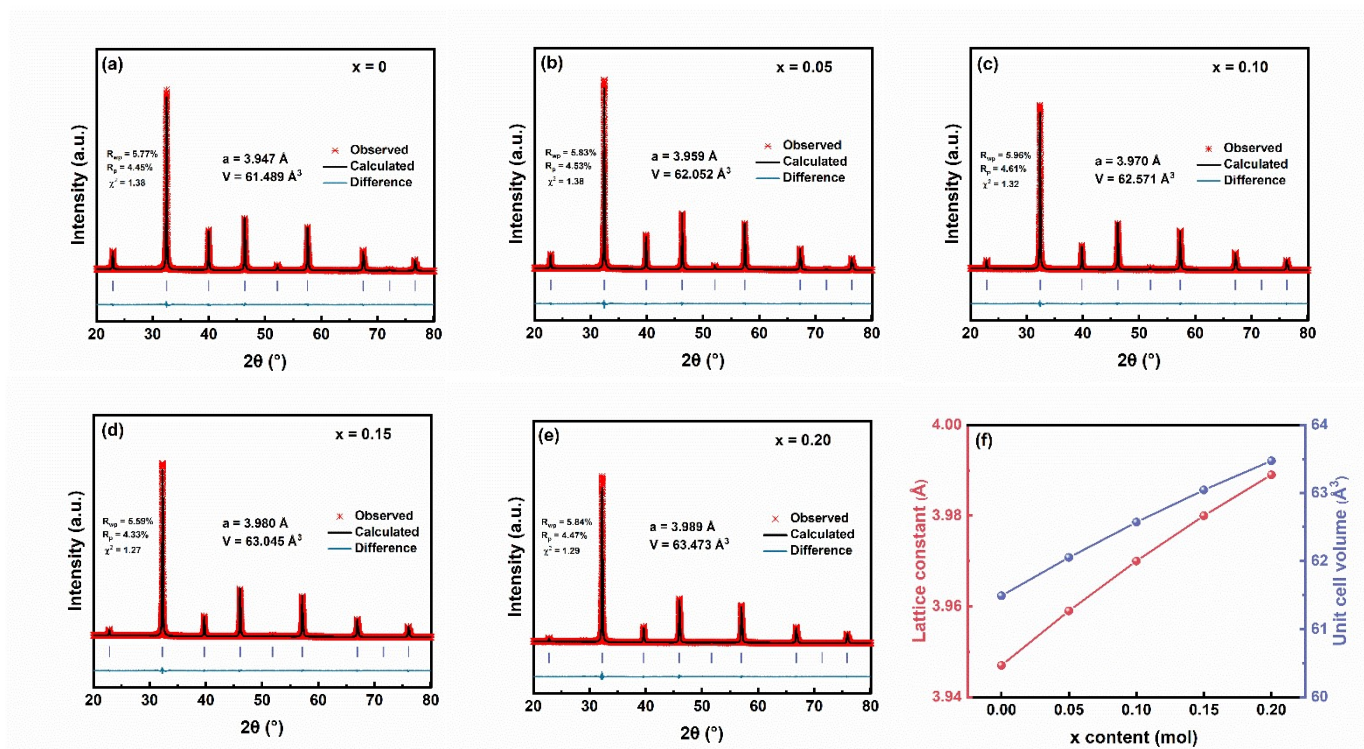


**Fig. S2** Refinement XRD patterns of BSBNTH ceramics: (a)  $x=0$ , (b)  $x=0.05$ , (c)  $x=0.10$ , (d)  $x=0.15$ , (e)  $x=0.20$ ; (f) The lattice constant and unit cell volume as functions of Hf content.

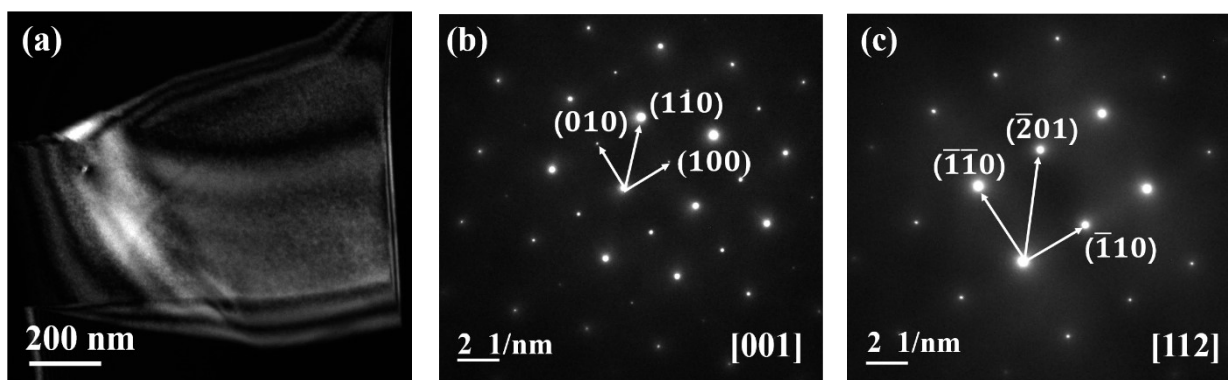


**Fig. S3** (a) Dark-field TEM image; The SAED spots along (b)  $[001]$  and (c)  $[112]$  for BSBNTH-15 ceramics.

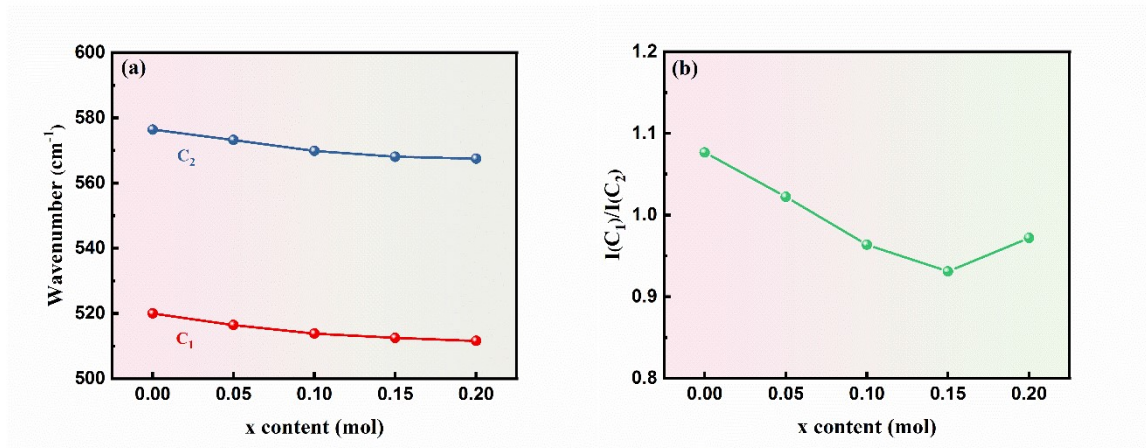


**Fig. S4** The evolution of the (a) wavenumber and (b) intensity ratio of the  $C_1$  and  $C_2$  as a function of Hf content in BSBNTH ceramics.

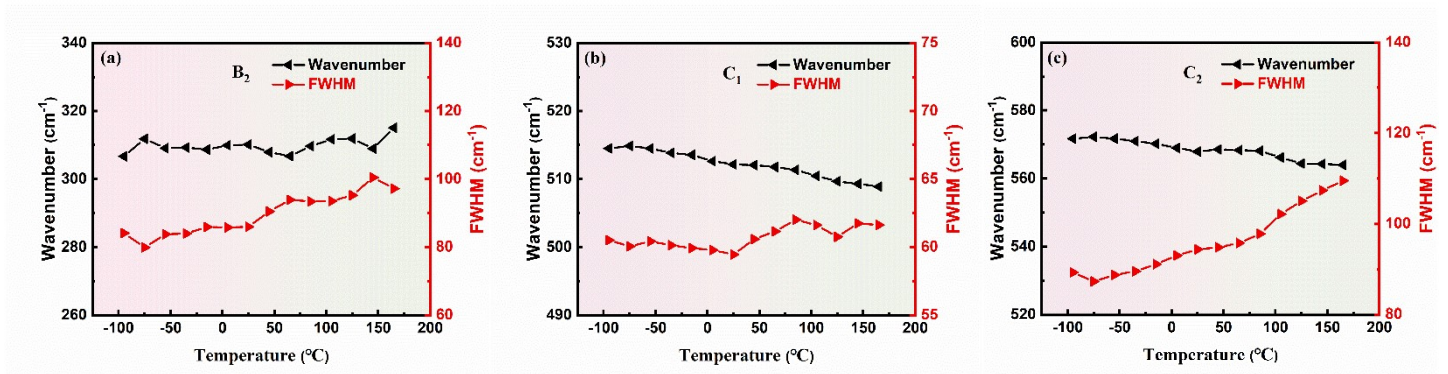


**Fig. S5** (a) The peak positions of Raman spectra from  $-95$  °C to  $165$  °C for  $x=0.15$  samples; the variance of wavenumber and full width at half maximum (FWHM) with increasing temperature for (b)  $B_2$ , (c)  $C_1$ , and (d)  $C_2$  Raman vibration modes.

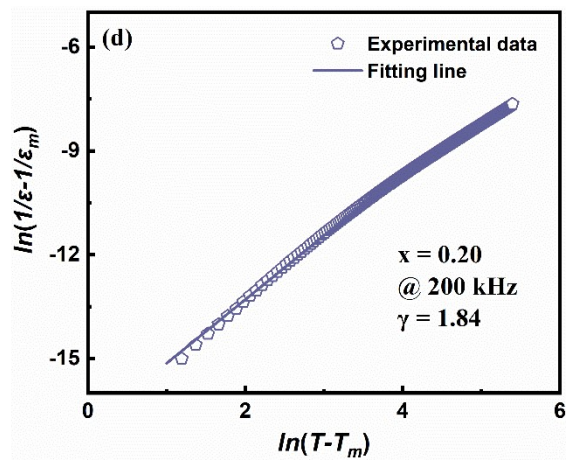
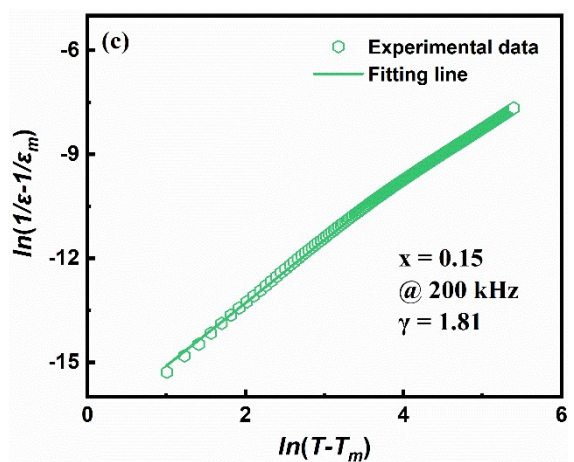
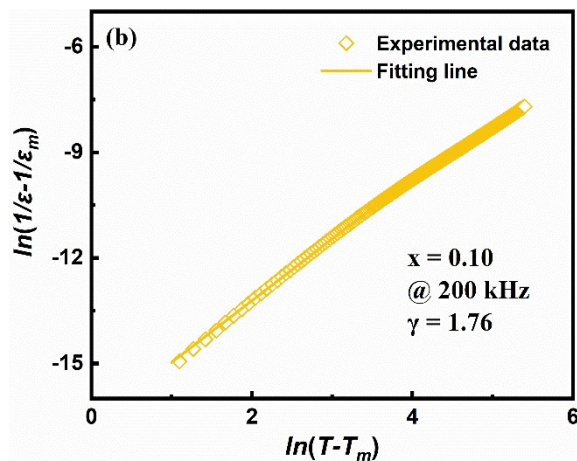
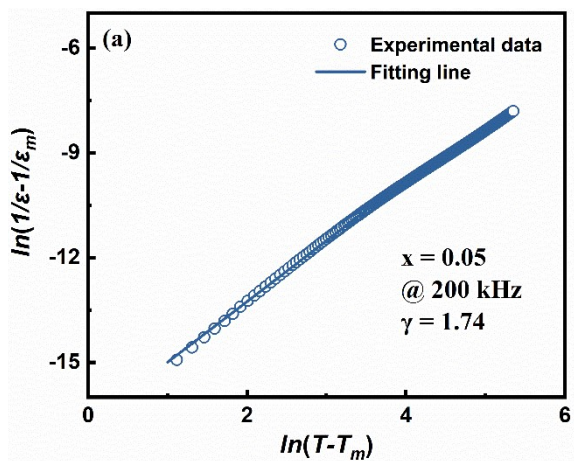


**Fig. S6**  $\ln(1/\varepsilon-1/\varepsilon_m)$  versus  $\ln(T-T_m)$  for BSBNTH ceramics: (a)  $x=0.05$ , (b)  $x=0.10$ , (c)  $x=0.15$ , (d)

$x=0.20$ .

**Table S1**

The relative dielectric constant and dielectric loss of BSBNTH ceramics measured at 25 °C and 1 kHz.

25 °C , 1 kHz	x=0	x=0.05	x=0.10	x=0.15	x=0.20
$\epsilon_r$	3427	2218	1505	1019	754
$\tan \delta$	0.05227	0.00492	0.00229	0.00131	0.00124

**Table S2**

The value of R and C is interpreted on an equivalent circuit with a parallel resistance capacitance (RC) element.

650°C	x=0	x=0.05	x=0.10	x=0.15	x=0.20
R ( $\Omega$ )	10991	20439	33275	34612	55363
C (F)	$5.51 \times 10^{-10}$	$5.79 \times 10^{-10}$	$4.83 \times 10^{-10}$	$4.18 \times 10^{-10}$	$3.74 \times 10^{-10}$

Compounds	E (kV/cm)	$W_{rec}$ (J/cm <sup>3</sup> )	$\eta$ (%)	ref
0.87BT-0.13Bi(Zn <sub>2/3</sub> (Nb,Ta) <sub>1/3</sub> )O <sub>3</sub>	218	1.44	92.5	[17]
0.88(Ba <sub>0.8</sub> Sr <sub>0.2</sub> )TiO <sub>3</sub> -0.12Bi(Zn <sub>2/3</sub> Nb <sub>1/3</sub> )O <sub>3</sub>	225	1.62	99.8	[60]
0.88BT-0.12Bi(Li <sub>0.5</sub> Nb <sub>0.5</sub> )O <sub>3</sub>	270	2.03	88.0	[58]
0.9BT-0.1Bi(Li <sub>0.5</sub> Ta <sub>0.5</sub> )O <sub>3</sub>	280	2.2	88.0	[59]
0.85BT-0.15Bi(Zn <sub>1/2</sub> Sn <sub>1/2</sub> )O <sub>3</sub>	280	2.41	91.6	[12]
0.85BT-0.15Bi(Mg <sub>0.5</sub> Zr <sub>0.5</sub> )O <sub>3</sub>	280	2.9	86.8	[56]
0.9Ba <sub>0.65</sub> Sr <sub>0.35</sub> TiO <sub>3</sub> -0.1BMN	400	3.34	85.7	[57]

BaTiO

?

-Bi(Mg

?.?

Zr

?.?

)O

?

345 3.41 85.1 [61]

BaTiO

?

-Bi(Mg

?.?

Zr

?.?

)0

?

<b>BaTiO<sub>3</sub>-Bi(Mg<sub>0.5</sub>Zr<sub>0.5</sub>)O<sub>3</sub>@SiO<sub>2</sub></b>				
<b>0.65(Ba<sub>0.98</sub>Li<sub>0.04</sub>)Ti<sub>0.98</sub>O<sub>3</sub>-0.35(Sr<sub>0.7</sub>Bi<sub>0.2</sub>)TiO<sub>3</sub></b>	<b>410</b>	<b>3.54</b>	<b>77.0</b>	<b>[54]</b>
<b>0.65BT-0.35(SBT-BMZ)</b>	<b>370</b>	<b>4.03</b>	<b>96.2</b>	<b>[53]</b>
<b>0.6(Ba<sub>0.75</sub>Sr<sub>0.25</sub>)TiO<sub>3</sub>-0.4Bi(Mg<sub>0.5</sub>Hf<sub>0.5</sub>)O<sub>3</sub></b>	<b>390</b>	<b>4.3</b>	<b>92.0</b>	<b>[14]</b>
<b>0.6BT-0.4Bi(Mg<sub>0.5</sub>Ti<sub>0.5</sub>)O<sub>3</sub></b>	<b>340</b>	<b>4.49</b>	<b>93.0</b>	<b>[16]</b>
<b>BT-0.06Bi<sub>2/3</sub>(Mg<sub>1/3</sub>Nb<sub>2/3</sub>)O<sub>3</sub></b>	<b>520</b>	<b>4.55</b>	<b>91.0</b>	<b>[15]</b>
<b>(Ba<sub>0.65</sub>Sr<sub>0.245</sub>Bi<sub>0.07</sub>)<sub>0.99</sub>Nd<sub>0.01</sub>TiO<sub>3</sub></b>	<b>460</b>	<b>4.2</b>	<b>76.0</b>	<b>[55]</b>
<b>This work</b>	<b>460</b>	<b>5.23</b>	<b>89.7</b>	
	<b>481</b>	<b>5.47</b>	<b>90.6</b>	

Table S3

Energy storage properties of BT-based ceramics



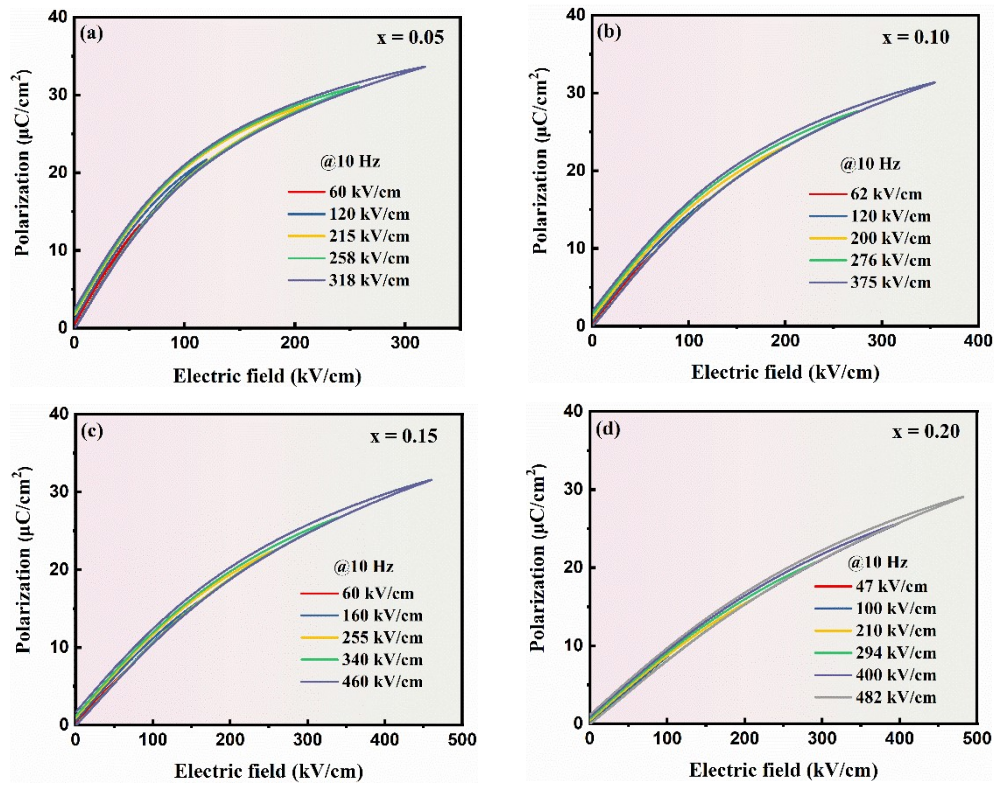


**Fig S7** Unipolar P-E loops of the BSBNTH ceramics at different electric fields: (a)  $x=0.05$ , (b)  $x=0.10$ , (c)  $x=0.15$ , (d)  $x=0.20$ .

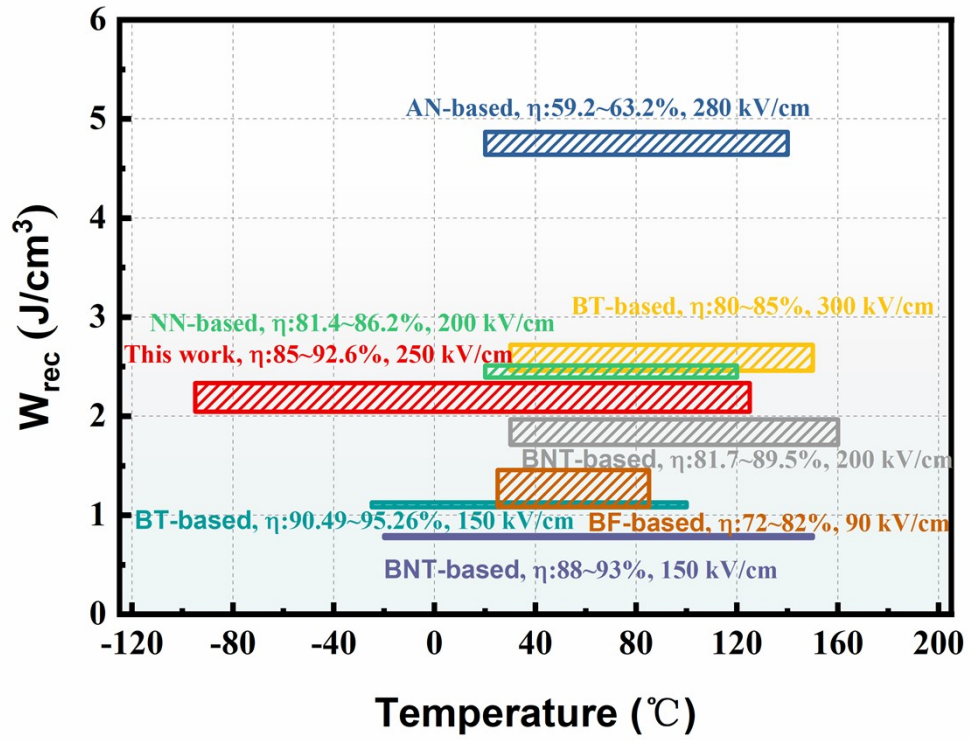


**Fig. S8** Temperature-dependent  $W_{rec}$  and  $\eta$  of the  $x = 0.15$  sample and recently reported lead-free ceramics (BT: BaTiO<sub>3</sub>, BF: BiFeO<sub>3</sub>, BNT: Bi<sub>0.5</sub>Na<sub>0.5</sub>TiO<sub>3</sub>, NN: NaNbO<sub>3</sub>, and AN: AgNbO<sub>3</sub>).

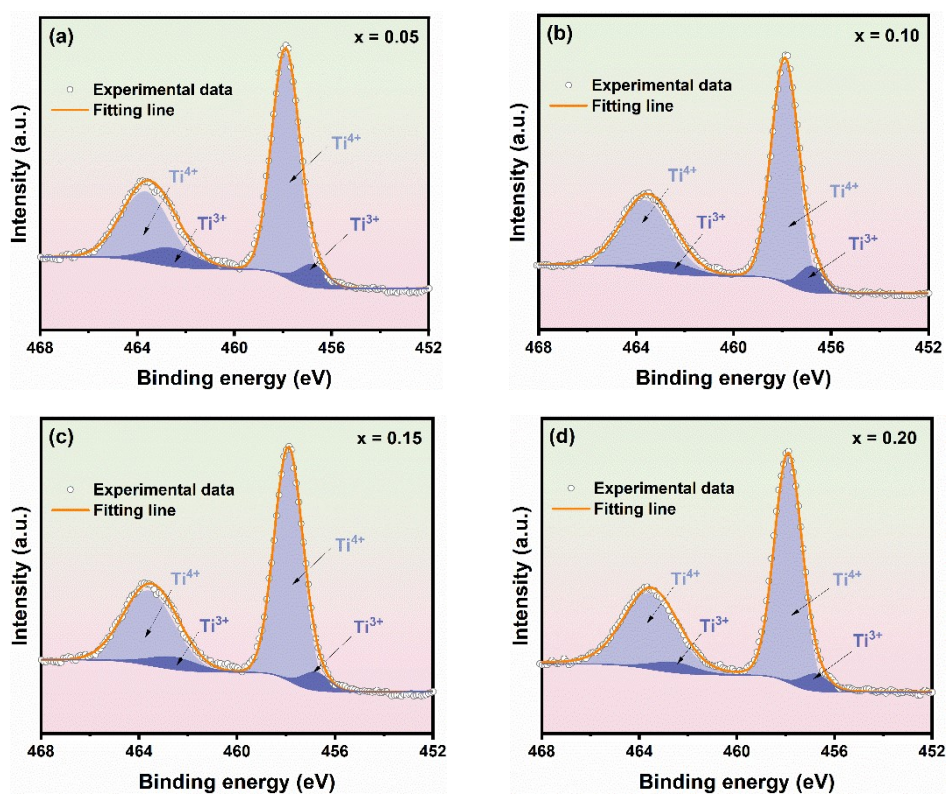
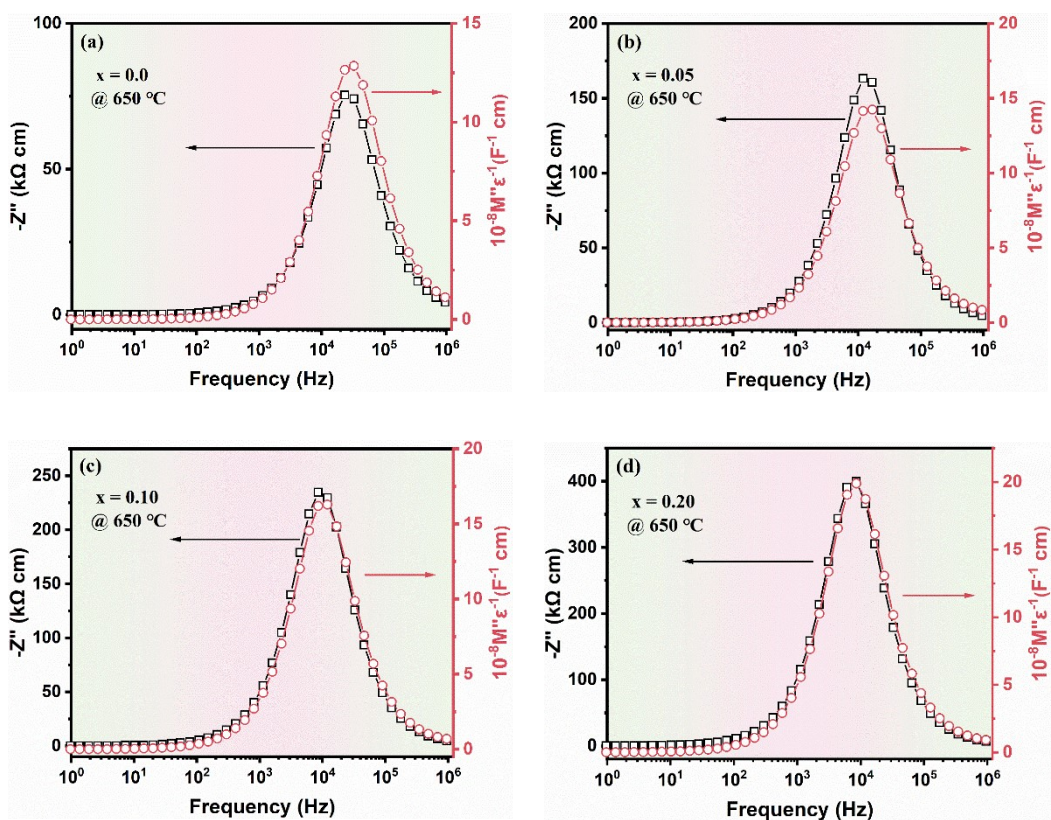


Fig. S9 XPS data of Ti 2p for BSBNTH ceramics: (a) x=0.05, (b) x=0.10, (c) x=0.15, (d) x=0.20.



**Fig. S10** Combined  $Z''$  and  $M''$  spectroscopic plots for BSBNTH ceramics: (a)  $x=0$ , (b)  $x=0.05$ , (c)  $x=0.10$ , (d)  $x=0.20$ .